35th EPS Conference on Plasma Phys. Hersonissos, 9 - 13 June 2008 ECA Vol.**32D**, P-5.149 (2008)

Electron Kinetic Effects And Beam-Related Instabilities In Hall Discharges: Relaxation Oscillations of the Sheath

D. Sydorenko and A. Smolyakov
Department of Physics and Engineering Physics,
University of Saskatchewan, Saskatoon, Saskatchewan S7N 5E2, Canada

I. Kaganovich and Y. Raitses
Princeton Plasma Physics Laboratory,
Princeton University, Princeton, New Jersey 08543, USA

Recent analytical studies and particle-in-cell simulations suggest that the electron velocity distribution function of a Hall thruster plasma is non-Maxwellian and anisotropic, resulting in many new properties of plasma in a Hall thruster. The present paper describes a regime of the discharge in which relaxation oscillations appear in the sheath near the thruster walls. The relaxation oscillations are observed in one-dimensional particle-in-cell simulations under the condition of intense turbulent heating. In this regime, the plasma switches between a state with non-space charge limited emission and a state with space charge limited emission. Transition to the latter state occurs when the negative conductivity appears due to the modification of the velocity distribution of the plasma bulk electrons.

Hall thrusters (HT), where plasma is maintained by an axial dc electric field crossed with a radial stationary magnetic field, are devices for spacecraft propulsion.[1] It is widely acknowledged that plasma-wall interaction strongly affects the HT operation.[2] Kinetic simulations reveal that the plasma potential, the sheath structure, and the intensity of plasma-wall interaction in HT are strongly affected by the non-Maxwellian electron velocity distribution function (EVDF), which is formed due to the nearly collisionless electron motion and intense secondary electron emission (SEE) from the walls.[3,4] Practical analytical formulas derived for wall fluxes, secondary electron fluxes, plasma parameters and conductivity in Ref. 5 agree well with the results of numerical simulations.

The authors use one-dimensional particle-in-cell (PIC) code[6] for simulation of Hall thruster plasmas in plane geometry, as shown schematically in Fig. 1. PIC simulation reveals a plasma-sheath instability manifesting itself as a rearrangement of the plasma sheath near the thruster channel walls accompanied by a sudden change of many discharge parameters. The instability develops when the sheath current as a function of the sheath voltage is in the negative conductivity regime. The description of the instability is given below.

Consider a PIC simulation of a thruster-like system carried out as follows. The constant simulation parameters are the distance between the walls $H = 2.5$ cm, the axial electric field $E_z = 200$ V/cm, the magnetic field $B_x = 100$ Gauss, the neutral xenon atom

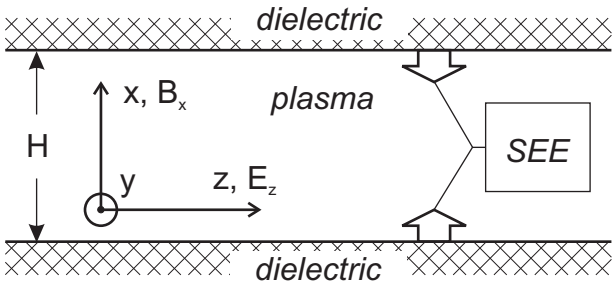

FIG. 1: Schematic diagram of the Hall thruster model. The two dielectric walls represent the coaxial ceramic channel of a Hall thruster.

density $N_a = 10^{12}$ cm^{-3}, and the turbulent collision frequency $\nu_t = 2.8 \cdot 10^6$ s^{-1}. Initially, the plasma (xenon) has uniform density $n_0 = 10^{11}$ cm^{-3} and isotropic electron temperature $T_{ex} = T_{ey} = T_{ez} = 10$ eV. The electron component has a drift in the y-direction with the velocity V_{dr}. The simulation parameters are not chosen so as to reproduce some regime of a real Hall thruster, but rather to investigate the plasma-wall interaction and the regime of the sheath with SEE while under the condition of intense turbulent heating. In particular, the space-charge limited (SCL) SEE regime[7] with $\gamma > \gamma_{cr}$ (for xenon plasma $\gamma_{cr} = 0.983$) and a non-monotonic potential profile in the sheath is expected.

In the simulation, the plasma becomes energetic and strongly anisotropic: $\langle w_y \rangle = 53$ eV, $\langle w_z \rangle = 42$ eV, $\langle w_x \rangle = 4.2$ eV, $\langle w_{y,z} \rangle \gg \langle w_x \rangle$, where averaging $\langle ... \rangle$ is done over all particles. The SCL SEE regime is observed in the simulation, but it never establishes as a stationary state. Instead, it is found that the system "switches" quasi-periodically between the SCL and non-SCL regimes. The SCL state lasts for a short time, while the non-SCL state lasts much longer (the width of the spikes in Fig. 2a is much smaller than the intervals between the spikes). In the SCL state, the primary electron flux grows abruptly and is several times higher than during the non-SCL state (see Fig. 2b) and the plasma potential decreases (see Fig. 2c).

In the SCL state, the electron energy losses at the walls are significantly enhanced compared to the non-SCL state, which strongly limits the electron energy. During the non-SCL state, the plasma replenishes the lost energy via the Joule heating. The dependence of the average electron energy versus time shown in Fig. 2d has a sawtooth shape, where the abrupt drops at the SCL state are followed by gradual increases during the non-SCL state. Note that in the minima of the energy curve in Fig. 2d the energy is still very high, $\langle w \rangle_{min} > 96$ eV, much higher than the critical electron temperature of transition to the SCL regime for a Maxwellian xenon plasma for the SEE properties of the chosen wall material, $T_{cr} \approx 18$ eV. The matter is that the energy in Fig. 2d is obtained by averaging over all electrons, while in RSO the periodic energy exchange occurs not for the whole EVDF, but rather for a certain part of it. If the plasma potential in the non-SCL state is Φ_p, and during the SCL state the potential drops by $\Delta\Phi < \Phi_p$, then the energy exchange will occur for particles with $\Phi_p - \Delta\Phi < w_x < \Phi_p$.

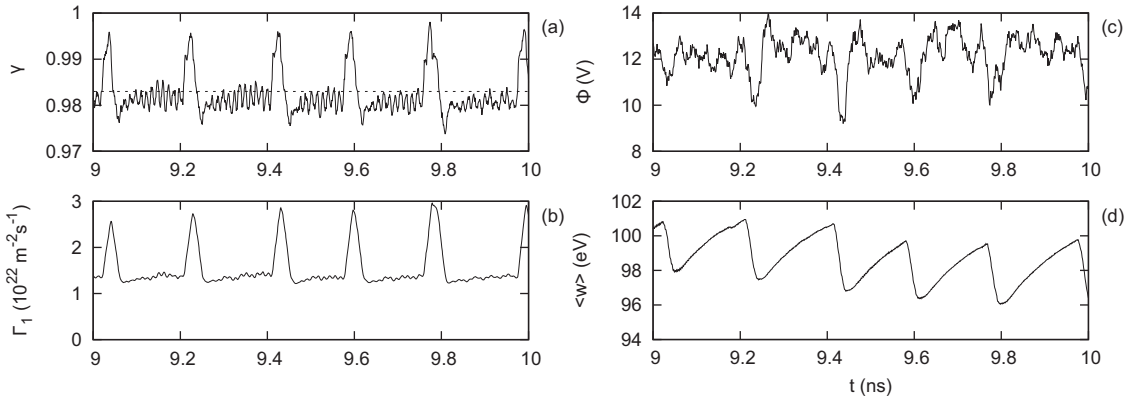

FIG. 2: Evolution of general plasma parameters with time in the RSO regime. (a) Total emission coefficient γ at the wall $x = L$ (red curve) and the threshold emission coefficient for the SCL SEE (blue line). (b) Total primary electron flux Γ_1 to the wall $x = L$. (c) Electrostatic potential in the middle of the plasma Φ_p. (d) Average electron energy $\langle w \rangle$.

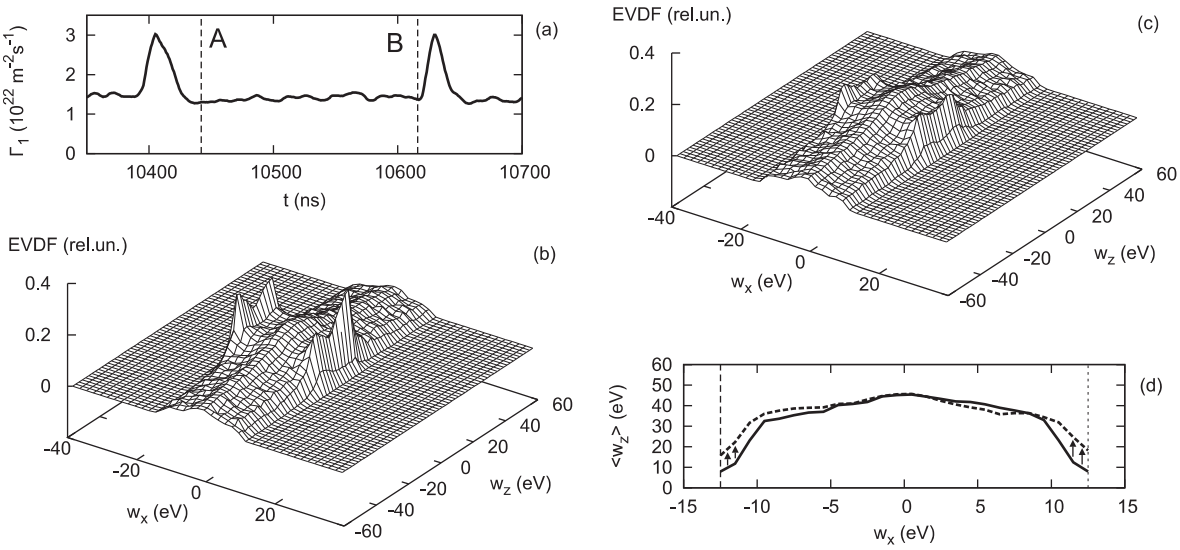

FIG. 3: (a) The primary electron flux to the wall $x = L$ during one RSO period, vertical lines A and B mark the beginning (time t_A) and the end (time t_B) of the non-SCL state. (b) and (c) The EVDF over v_x and v_z in the middle of the plasma 10 mm $< x <$ 15 mm obtained at t_A (b) and t_B (c). (d) The dependence $\langle w_z \rangle (v_x)$ at t_A (solid curve) and t_B (dashed curve). Vertical lines in (d) mark the electron confinement threshold $e\Phi_p$. Graphs in (b), (c), and (d) are plotted in energy coordinates, negative energy values correspond to propagation in the negative direction.

In Fig. 3(b) and (c), we represent the bulk plasma electron distribution function over the x and z velocities in the midplane, $f(v_x, v_y, H/2)$, obtained during the non-SCL stage of one RSO period shown in Fig. 3(a). At the time t_A marked by vertical line A in Fig. 3(a), which is immediately after the end of the SCL stage, the EVDF has high-

amplitude spikes created by numerous *cold* secondary electrons trapped by the restored plasma potential, see Fig. 3(b). With time, these spikes disperse, because electrons (i) suffer turbulent collisions (the anisotropic Joule heating), and (ii) are mixed in the phase space x-v_x by a weak two-stream instability[8]. By the end of the non-SCL stage (time t_B) marked by vertical line B in Fig. 3(a), the amplitude of the spikes in the EVDF decreases by a factor of two, see Fig. 3(c). To give a quantitative characteristic of the local EVDF modification, in Fig. 3d we plotted dependencies of mean energy in the x-direction $\langle w_z \rangle (v_x)$ for the plasma trapped bulk electrons with $w_x < e\Phi_p$ at times t_A and t_B, in the discharge center $x = H/2$. The dashed curve $\langle w_z \rangle (v_x)$ obtained at time t_B is clearly higher than the solid curve obtained at time t_A in the region 10 eV $< w_x <$ 12.5 eV. In other words, by the end of the non-SCL stage, the electrons with $\Phi_p - \Delta\Phi < w_x < \Phi_p$ significantly increase their energy of motion parallel to the walls. This energy becomes the source for the upcoming SCL stage.

It is interesting that although the emission coefficient γ gradually increases during the non-SCL stage, the transition to the SCL stage with $\gamma > \gamma_{cr}$ occurs in a jump-like manner at the moment when γ is still below γ_{cr}. Such behavior is typical for unstable systems and can be explained by the modification of the current-voltage characteristic of the sheath related with the modification of the EVDF during the non-SCL stage described above.

Simulations were carried out using the Westgrid facilities in the University of British Columbia.

---

[1] V. V. Zhurin, H. R. Kaufman, and R. S. Robinson, Plasma Sources Sci. Technol. **8**, R1 (1999).

[2] Y. Raitses, D. Staack, M. Keidar, and N. J. Fisch, Phys. Plasmas **12**, 057104 (2005).

[3] D. Sydorenko, A. Smolyakov, I. Kaganovich, and Y. Raitses, Phys. Plasmas **13**, 014501 (2006).

[4] D. Sydorenko, A. Smolyakov, I. Kaganovich, and Y. Raitses, Phys. Plasmas **15**, 053506 (2008).

[5] I. Kaganovich, Y. Raitses, D. Sydorenko, and A. Smolyakov, Phys. Plasmas **14**, 057104 (2007).

[6] D. Sydorenko, Ph.D. thesis, University of Saskatchewan (2006), http://library2.usask.ca/theses/available/etd-06142006-111353.

[7] G. D. Hobbs and J. A. Wesson, Plasma Phys. **9**, 85 (1967).

[8] D. Sydorenko, A. Smolyakov, I. Kaganovich, and Y. Raitses, Phys. Plasmas **14**, 013508 (2007).